Taylor & Francis
Taylor & Francis Group

Synthesis and Property of Polypyrrole/Multi-Walled Carbon Nanotube Nanocomposites in Supercritical Carbon Dioxide

HALDORAI YUVARAJ,[1] YEON TAE JEONG,[1]
HYUN GYU KIM,[2] YEONG SOON GAL,[3]
SEONG-SOO HONG,[4] AND KWON TAEK LIM[1]

[1]Department of Image System Engineering, Pukyong National University, Busan, Korea
[2]Korea Basic Science Institute, Busan Centre, Busan, Korea
[3]Division of Polymer Chemistry Laboratory, Kyungil University, Kyungsan, Korea
[4]Division of Applied Chemical Engineering, Pukyong National University, Busan, Korea

Electrically semiconducting polypyrrole/multi-walled carbon nanotube (PPy/MWNTs) composites were prepared by in-situ *oxidative polymerization of pyrrole in the presence of MWNTs in supercritical carbon dioxide (scCO$_2$). Prior to the polymerization, MWNTs were surface modified with silane coupling agent 3-(trimethoxysilyl) propyl methacrylate in order to be dispersed well in scCO$_2$. TEM and FESEM analysis showed that a tubular layer of PPy film is coated on the MWNTs surfaces, which were a few nanometers in thickness. The incorporation of MWNTs in the composite was endorsed by FT-IR. The composites were also confirmed by XRD and XPS. The composites synthesized in scCO$_2$ were shown to possess higher thermal stability and electrical conductivity than PPy. Additionally, the dispersibility of the composite in ethanol was also demonstrated.*

Keywords Carbon nanotube; composite; polypyrrole; supercritical CO$_2$; surface modification

Introduction

Since their discovery, carbon nanotubes (CNTs) [1] have been a focus of considerable research interest due to their potential applications. Their unique properties include their interesting mechanical, thermal and electrical conductivity behavior; they offer tremendous opportunities for the development of fundamentally new material systems for application in nano-electronic devices [2,3], scanning probe

Address correspondence to Prof. Kwon Taek Lim, Department of Image System Engineering, Pukyong National University, San 100 Yongdang-Dong, Nam-Gu, Busan 608-739, Korea (ROK). Tel.: (+82)51-629-6309; Fax: (+82)51-629-6409; E-mail: ktlim@pknu.ac.kr

microscopy [4], field emitters [5] and so forth. Similarly, composites based on polymers and nanotubes have the potential to make an impact on a variety of applications ranging from general low-cost circuits and displays to power devices, micro-electromechanical systems, super capacitors and solar cell sensors [6,7]. Despite their appealing properties, the low dispersibility of CNTs in most organic solvents and their poor compatibility within a polymer matrix makes the uniform dispersion of carbon nanotubes in the polymer matrix very difficult, which limits their applications. Nanotube dispersion into polymers can be improved by either using surfactants as processing aids [8], functionalization [9] and *in-situ* polymerization [10].

The ability to combine CNTs with conducting matrices such as poly(3-octylthiophene) [11] poly(3,4-ethylenedioxythiophene) [12] and poly(*p*-phenylene vinylene) [13] to produce nanocomposite materials has stimulated much research interest, particularly in organic electronics. Among the conducting polymers, polypyrrole (PPy) is one of the most important conducting polymers because of its relatively facile processability, electrical conductivity and environmental stability. Synthesis and characterization of PPy/CNT composites have been reported by a number of authors in the literature [14–20]. Diverse chemical methodologies have also been developed to synthesize conducting polymer/CNT composites. However, processing of polymers generally employs large quantity of organic solvents that are noxious and harmful to the environment. Thus, processing with a supercritical fluid such as carbon dioxide offers an attractive alternative to the conventional processing.

We focused on designing a method that will replace "wet" processes based on water and organic solvents with "dry" processes based on the use of supercritical carbon dioxide (scCO$_2$). Compressed carbon dioxide is a promising alternative solvent for such manufacturing methods since it is environmentally benign, inexpensive and easily recyclable. Products can be easily isolated as a dry powder by simple depressurization of CO$_2$. Moreover supercritical CO$_2$ has a strong solvent power for dissolving some organic compounds and a swelling property for most organic polymers [21]. On the other hand, CO$_2$ acts as an anti-solvent because the solvent power of CO$_2$ is much weaker than that of organic solvents for many solutes. The special properties of scCO$_2$ have been used to fabricate nanomaterials [22,23] which are difficult to prepare by traditional techniques. Recently, Dai and co-workers [24] synthesized carbon nanotube/poly(2,4-hexadiyne-1,6-diol) nanocomposites with the aid of scCO$_2$/ethanol co-solvent mixture. But they failed to disperse multi-walled carbon nanotubes (MWNTs) in scCO$_2$, which usually leads to the formation of large aggregates. It is necessary to disperse nanotubes prier to the polymerization in order to increase the mechanical, thermal and electrical properties of the composite materials. More recently Yue *et al.* synthesized PMMA/SWNT nanocomposites by dispersion polymerization in scCO$_2$ [25]. To our knowledge no study has been reported in the synthesis of well dispersed CNTs and conjugated conducting polymer composites in scCO$_2$. In this report, we demonstrate a facile one-pot synthesis of PPy/MWNTs composites in scCO$_2$ by *in-situ* oxidative polymerization of pyrrole in the presence of siliane coupling agent (3-(trimethoxysilyl) propyl methacrylate, MPS) modified nanotubes. The morphology, structure, thermal properties and conductivity are reported for these composites with varying MWNTs concentration. This environmentally benign green synthetic route offers advantages of easy separation and resolves problems related to solvent removal.

Experimental

Materials

Pyrrole (Aldrich) was purified using a column of activated basic alumina. The MWNTs synthesized by a catalytic chemical vapor deposition method were purchased from Aldrich (>90% pure). The MWNTs have a diameter of 10–20 nm and length of 0.1–10 μm. Hydrochloric acid (Aldrich), potassium permanganate (Aldrich), tetrapropyl ammonium bromide (TPABr) (Aldrich), acetic acid (Aldrich), 3-(trimethoxysilyl) propyl methacrylate (MPS, Aldrich), methanol (Aldrich), ferric chloride (Aldrich) and research-grade CO_2 (Daeyoung Co., 99.99%) were used as received. Methylene chloride (Aldrich) and toluene (Aldrich) were distilled over CaH_2 prior to use.

Grafting of hydroxyl groups on the surface of MWNTs.

MWNTs were treated with 35% HCl at 55°C for 5 h prior to the experiment in order to remove impurities such as amorphous carbon and metallic catalyst present. MWNTs (0.5 g) and 300 mL methylene chloride were placed in a 500 mL flask, and the mixture was dispersed by ultrasonication (Branson-5210) for 30 min. TPABr (2 g) and $KMnO_4$ (2 g) dissolved in 20 mL H_2O and 20 mL acetic acid solution were added into the flask. The mixture was stirred vigorously at room temperature for 24 h. Then it was washed with HCl followed by methanol (methanol washing step was repeated at least five times) and filtered through a 0.2 μm PTFE membrane filter (Adventec MFS). After vacuum drying the filtrate, 0.4 g of hydroxyl group functionalized MWNTs (MWNTs-OH) were obtained.

Synthesis of MPS Modified MWNTs

After dispersing 0.4 g of MWNTs-OH in 100 mL toluene by ultrasonication for 30 min, an excess of MPS was added. The resulting solution was stirred at 65°C for 24 h under argon atmosphere. The product was isolated by centrifugation and washed repeatedly with methanol to remove residual MPS. Finally it was dried at 60°C under vacuum for 24 h.

Synthesis of PPy/MWNT Composite in scCO₂

In a typical experiment, 0.05 g of MPS modified MWNTs was dispersed into 1 g of pyrrole under sonication for 30 min to form a suspension, and then the black suspension was moved into a 40 mL high-pressure reactor vessel. A required amount of ferric chloride dissolved in methanol was added into the vessel. The reactor was sealed, and densified CO_2 was introduced using an ISCO syringe pump (260 D) at 40°C and 103 bar. The *in-situ* polymerization was carried out with the stirring speed of 700 rpm for about 4 h, and then the vessel was cooled to room temperature. The resulting precipitate was collected and repeatedly washed with methanol and distilled water to remove the oxidant. Finally, the sample was dried at 60°C under vacuum for 24 h.
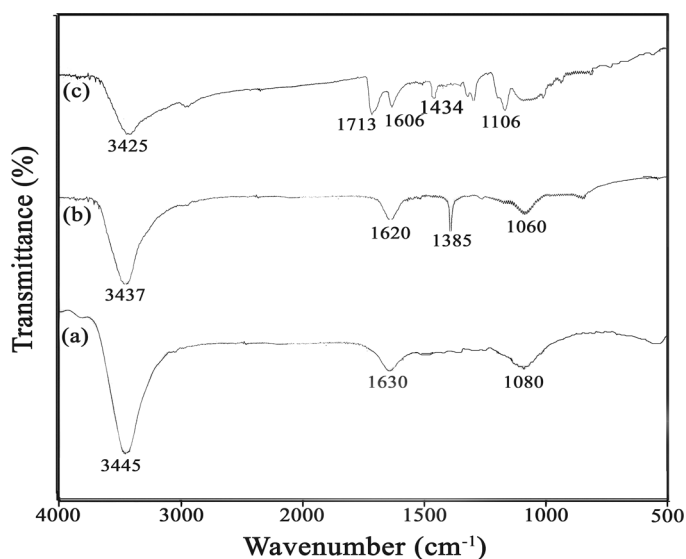
Characterization

FT-IR characterizations were performed using a BOMEM Hartman & Braun spectrometer. TEM images were obtained on a transmission electron microscope (JEOL,

JEM-2010) operated with an accelerating voltage of 200 kV. Microscopic pictures of composites were obtained by a Hitachi S-2400 field emission scanning electron microscope (FESEM). Thermal stability was investigated by thermal gravimetric analyzer (Perkin Elmer, TGA-7) under a nitrogen flow (35 mL/min). The heating rate was 10°C/min. The XRD patterns were collected on a powder X-ray diffract-ometer (Philips, X'Pert-MPD) with Cu Ka radiation. X-ray photoelectron spec-troscopy (XPS) measurements were performed with a multilab 2000 electron spectrometer with an Al X-ray source. The room temperature conductivity of the pressed pellets was measured by the SBY-4 four-point probe apparatus.

Results and Discussion

In order to obtain PPy/MWNT composites in scCO$_2$, it is necessary to disperse MWNTs prior to the polymerization. The MWNTs could be dispersed in scCO$_2$ after surface modification with the siliane coupling agent MPS, which is due to the favorable interaction between MPS molecules and CO$_2$ [26]. The surface modi-fication of MWNTs was carried out according to the previous literature protocol [27]. Figure 1 shows the FT-IR results of the MWNTs obtained at different proces-sing steps. For the pristine MWNTs (Fig. 1a), the bands at 3445 and 1080 cm^{-1} are attributed to the presence of hydroxyl groups (−OH) on the surface of MWNTs, which are believed to result from either ambient atmospheric moisture bound to the MWNTs or oxidation during purification of the raw material [28]. Another band at 1630 cm^{-1} is assigned to the C=O stretching of quinone groups on the surface of MWNTs. The spectrum of the hydroxyl groups functionalized MWNTs (Fig. 1b), was verified by the appearance of a band at 1385 cm^{-1}, which is assignable to the bending vibration of the –OH group [29]. In the MPS functionalized MWNTs (Fig. 1c), the band at 3425 cm^{-1} became broader and weaker, and the band at


Figure 1. FT-IR spectra of the MWNTs (a) pristine, (b) hydroxyl functionalized and (c) MPS grafted.

$1385\,cm^{-1}$ almost disappeared. On the other hand, the characteristic absorption bands at CH_3 ($1434\,cm^{-1}$), $C=O$ ($\sim1713\,cm^{-1}$), $C=C$ ($\sim1606\,cm^{-1}$) and Si–O–Si ($\sim1106\,cm^{-1}$) indicate the availability of silane group on the surface of MWNTs [29].

The principle procedure involved in the synthesis of PPy/MWNTs composites consists of two steps. The first step is the surface grafting of MWNTs by MPS. Finally, the *in-situ* oxidative polymerization of pyrrole is carried out in the presence of surface grafted MWNTs in $scCO_2$. Polymerization reactions were carried out with varying ratio of MWNTs (2.5 to 10% w/w) to pyrrole in $scCO_2$. The FESEM pictures of PPy, MWNTs and 2.5% composite are presented in Figure 2. The MWNTs have tubular network structure both in the pure state and in the composites. From Figure 2a, one can see that the bulk PPy (synthesized without MWNTs) shows a typical morphology. The pristine MWNTs morphology is also displayed in Figure 2b, and the diameter of each nanotube is about 10–20 nm. In Figure 2c, PPy is tightly coated onto the surface of each nanotube; many neighboring MWNTs are joined together with the semiconducting polymer at a variety of angles. To ascertain the physical nature of the MWNTs in the composites more clearly, the TEM images of MWNTs and composites are presented in Figure 3a–d. The MWNTs sample is clearly evident in the image (Fig. 3a) as endless, tangled, hollow ropes with smooth surface. It is important to note that the MWNTs are fatter in all the composites than those in the pure sample. From Figure 3b it is apparent that the MWNTs of 2.5% composite have a thicker outer diameter (65 nm) than that of the pure
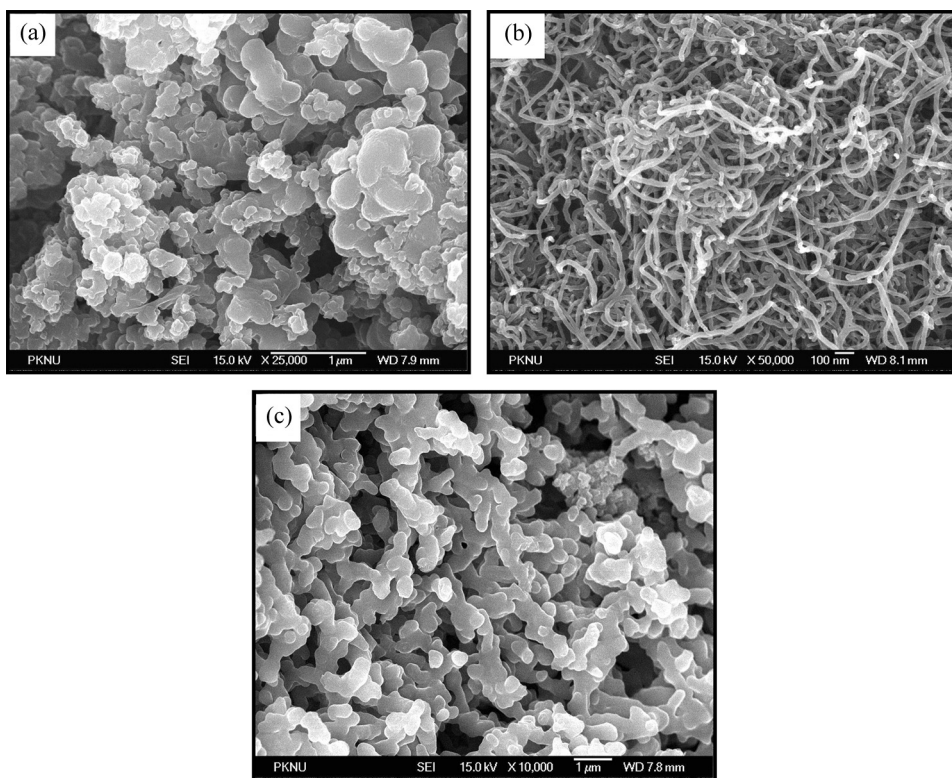
Figure 2. FESEM pictures of (a) PPy, (b) MWNTs and (c) 2.5% composite.
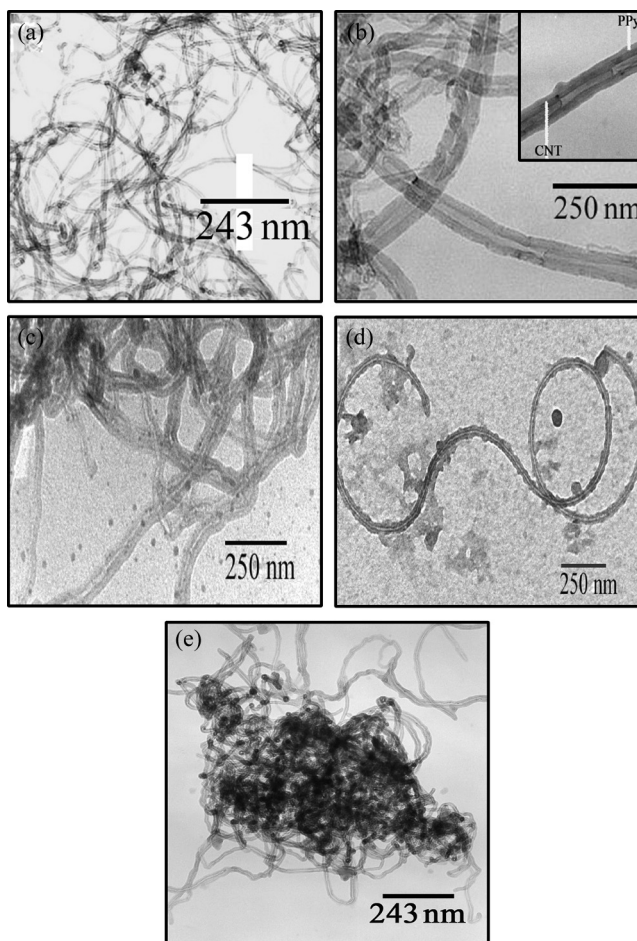
Figure 3. TEM images of (a) MWNTs, (b) 2.5% composite, (c) 5% composite, (d) 10% composite and (e) 2.5% composite (pristine).

sample. This is also true for other composites; e.g., for 5% composite the average outer diameter is 45 nm, and for 10% composite it is 31 nm. Thus, from the increase of thickness of outer diameter it can be inferred that the larger the concentration of MWNTs, lower is the degree of wrapping. This study therefore concludes that the surface of MWNTs is well wrapped by the polymer. The inset of Figure 3b presents the close inspection of the composite. This Figure clearly put evidence that the MWNTs of darker contrast are wrapped by the PPy of lighter contrast. For comparison, PPy/MWNTs (pristine) composites were also prepared under precisely the same condition. Untreated MWNTs did not form a good suspension in the monomer even with sonication. In addition, MWNTs did not disperse in the reaction medium. Figure 3e displays the TEM image of PPy/MWNTs (pristine) composites showing that the pristine MWNTs were primarily coated by the polymer in the form of large aggregates with essentially no dispersion. In Figures 3a–d the surface of the nanotubes is smooth, but in Figure 3e the surface of the nanotubes is full of protuberance. These spheroid-like particles on the nanotubes surface indicate that the
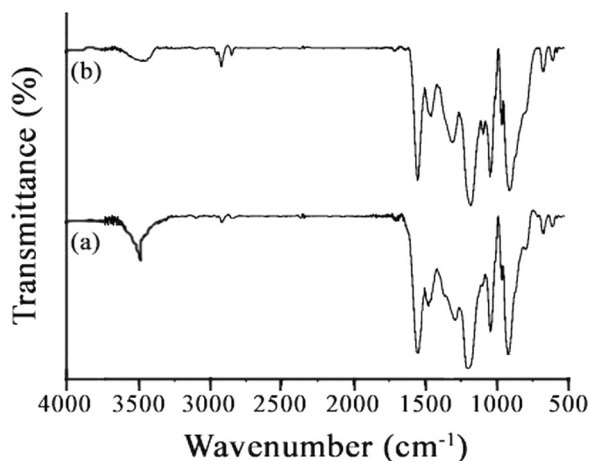
Figure 4. FT-IR spectra of (a) PPy and (b) 2.5% composite.

MWNTs are not completely wrapped by the polymer and some portions remain phase separated.

Figure 4 illustrates the FT-IR spectra of PPy and PPy/MWNTs (2.5%) composites. It is clear that the PPy and composites showed very similar spectra. The strong peaks at 1564 and 1474 cm^{-1} were attributed to the antisymmetric and symmetric ring-stretching modes of PPy [14], while the peaks at 1305 and 1043 cm^{-1} were due to C−N stretching vibrations and C−H deformation vibrations of PPy, respectively [30]. The strong peaks near 1210 and 925 cm^{-1} indicate the doping state of PPy [18]. A broad band centered at 3402 cm^{-1}, due to the characteristic N−H stretching vibration, suggests the presence of secondary amino groups and becomes weaker with an increase in the content of MWNTs.

Figure 5 shows the TGA curves of MWNTs, PPy and 10% composite under nitrogen atmosphere. It can be seen that MWNTs were stable and did not show a dramatic decomposition in the tested temperature range. PPy showed around ca.
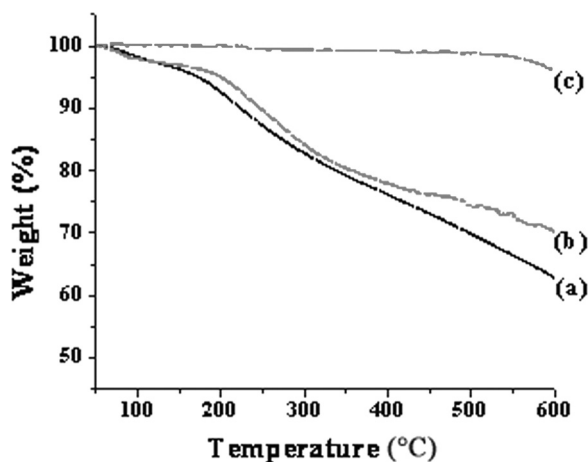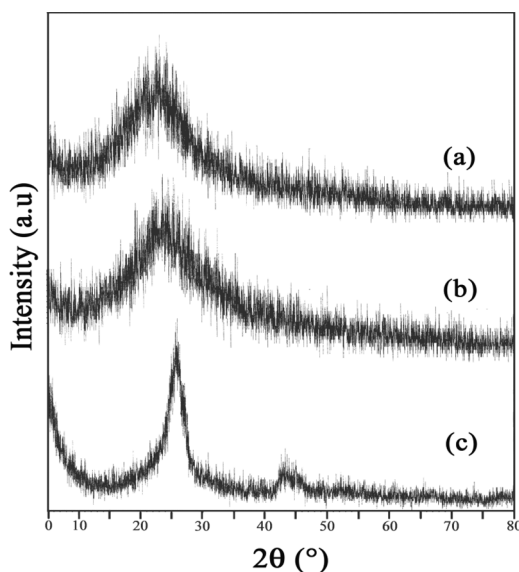

Figure 5. TGA curves of (a) PPy, (b) 10% composite, and (c) MWNTs in nitrogen.

**Figure 6.** XRD patterns of (a) PPy, (b) 2.5% composite, and (c) MWNTs.

14% mass loss until 250°C, but a rapid mass loss occurred at higher temperature. The mass remained for the composites is higher than that of the bare polymer at temperatures higher than 250°C, which was obviously related to the existence of thermally stable MWNTs.

XRD patterns of MWNTs, PPy and their 2.5% composites were depicted in Figure 6. Two peaks were observed at 2θ values of 25.8° and 43.3° in the spectrum of MWNTs, which were attributed to a graphite-like structure [18]. In contrast, no peaks were observed in the spectrum of PPy, suggesting an amorphous structure of the polymer prepared by *in-situ* oxidative polymerization. The XRD pattern of the composite was very similar to that of PPy alone, indicating that no additional crystalline order or chain arrangement had been introduced into the composites. The results revealed that a layer of very thin film was formed on the surface of MWNTs in the process of polymerization. While the appearance of a small peak at 2θ value of 25.9° suggested the existence of MWNTs in the composites.

Figure 7 shows the XPS analysis of bulk PPy powder, 2.5% composite, and pristine MWNTs. There is no N-1s spectrum in the case of MWNTs whereas the N-1s spectrum of the bulk PPy showed two peaks at a binding energy of about 396.5 eV, which is characteristic of the amine-like or neutral pyrrolium nitrogen (−NH− structure). A high-binding energy at about 400.1 eV is attributable to the positively charged nitrogen (−N$^+$H− structure) [31]. The N-1s spectrum of the composites is also at the same position. It means that the chemical environment of the N element, in the pure polymer and the composites is almost identical. Similarly, in the case of C−1s, the core-level spectra of the polymer and composites also showed very similar results.

The electrical conductivity measurements of PPy, MWNTs, and PPy/MWNTs composites were carried out using a four-point probe apparatus, and the room-temperature conductivities of the above mentioned materials are presented in Table 1. Apparently, the conductivity increases with an increasing fraction of
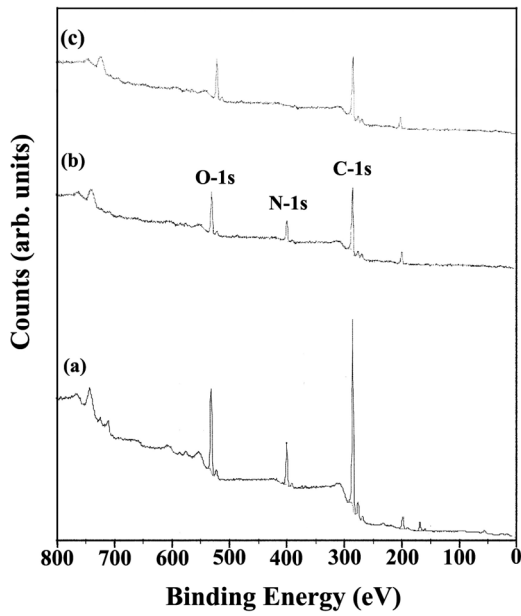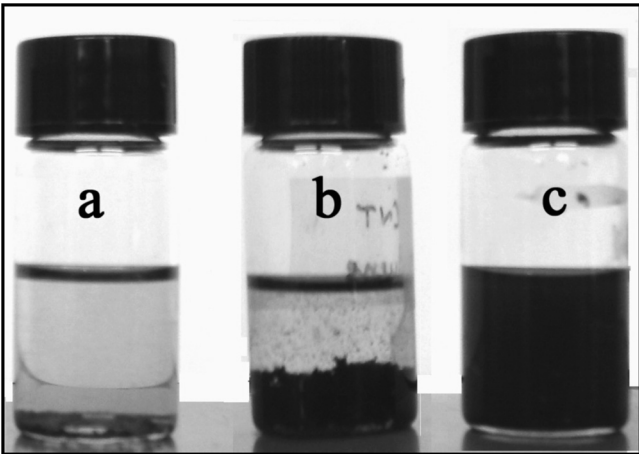
Figure 7. Survey XPS spectrum of (a) PPy, (b) 2.5% composite, and (c) MWNTs.

Table 1. The room-temperature conductivities of PPy/MWNTs composites

Samples	MWNTs	PPy	2.5% composite	5% composite	10% composite
Conductivity (S/cm)	6.24	3.05×10^{-2}	3.40×10^{-1}	4.75×10^{-1}	6.41×10^{-1}

Figure 8. Suspension stability of (a) MWNTs, (b) surface functionalized MWNTs, and (c) 2.5% composite in ethanol.

MWNTs. The conductivity of pure PPy is 3.05×10^{-2} S/cm (the room-temperature conductivity of MWNTs is 6.24 S/cm). However, the conductivity of the PPy/MWNTs composite is increased to 3.40×10^{-1} S/cm (one order magnitude) by introduction of 2.5% MWNTs. Generally in the semiconducting polymer nanocomposites, the conductivity depends not only on the doping level, conjugated length, or chain length but also on some external factors such as the compactness of the sample or orientation of the polymer particles [32].

In order to compare the suspension stability of the MWNTs, surface functionalized MWNTs and 2.5% composites in ethanol solutions with a sample concentration of 0.5 mg/ml were prepared. Figure 8 shows the results of the suspending states of the MWNTs samples after 10 min of dispersion via sonication. Comparison of these photographs indicates that the suspension stability of the pristine MWNTs (Fig. 8a) was poor: they easily sedimented in ethanol due to the agglomeration and poor hydrogen-bonding ability. On the other hand, as can be seen in Figure 8b, the surface functionalized MWNTs showed better stability than the pristine MWNTs and phase separation occurred after long time. However, composites presented the best stability (Fig. 8c). The homogeneous black color in the system was direct evidence for the existence of MWNTs wrapped polymer in the solution.

Conclusions

PPy/MWNTs composites were prepared by *in-situ* oxidative polymerization of pyrrole in the presence of MPS modified MWNTs in scCO$_2$. FESEM and TEM analyses proved that the MWNTs were homogeneously dispersed in the polymer matrix. The composites showed high thermal stability in comparison with pure PPy. The room-temperature conductivity increased with an increase in the fraction of MWNTs in the composites. The surface modified MWNTs and composites showed good dispersibility in ethanol.

Acknowledgments

References

[1] Iijima, S., & Ichihashi, T. (1993). *Nature*, *363*, 603.
[2] Fan, S., Chapline, M. G., Franklin, N. R., Tombler, T. W., Cassell, A. M., & Dai, H. (1999). *Science*, *283*, 512.
[3] Frank, S., Poncharal, P., Wang, Z. L., & de Heer, W. A. (1998). *Science*, *280*, 1744.
[4] Tans, S. J., Verschueren, A. R. M., & Dekker, C. (1998). *Nature*, *393*, 49.
[5] Dai, H., Hafner, J. H., Rinzler, A. G., Colbert, D. T., & Smalley, R. E. (1996). *Nature*, *384*, 147.
[6] Williams, O. A., Whitfield, M. D., Jackman, R. B., Foord, J. S., Butler, J. E., & Nebel, C. E. (2001). *J. Appl. Phys. Lett.*, *78*, 3460.
[7] Kleinsorge, B., Ferrari, A. C., Robertson, J., & Milne, W. I. (2000). *J. Appl. Phys.*, *88*, 1149.
[8] Gong, X., Liu, J., Baskaran, S., Voise, R. D., & Young, J. S. (2000). *Chem. Mater.*, *12*, 1049.

[9] Georgakilas, V., Kordatos, K., Prato, M., Guldi, D. M., Hoizinger, M., & Hirsch, A. (2002). *J. Am. Chem. Soc.*, *124*, 760.

[10] Tang, Z., & Xu, H. (1999). *Macromolecules*, *32*, 2569.

[11] Kymakis, E., & Amaratunga, G. A. (2002). *J. Appl. Phys. Lett.*, *80*, 112.

[12] Woo, H. S., Czerw, R., Webster, S., Carroll, D. L., Park, J. W., & Lee, J. H. (2001). *Synth. Met.*, *116*, 369.

[13] Ago, H., Petritsch, K., Shaffer, M. S. P., Windle, A. H., & Friend, R. H. (1999). *Adv. Mater.*, *11*, 1281.

[14] Zhang, X., Zhang, T., & Liu, Z. (2005). *Carbon*, *43*, 2186.

[15] Yu, Y., Ouyang, C., Gao, Y., Si, Z., Chen, W., Wang, Z., & Xue, G. (2005). *J. Polym. Sci. Part A: Polym. Chem.*, *43*, 6105.

[16] An, K. H., Jeong, S. Y., Hwang, H. R., & Lee, Y. H. (2004). *Adv. Mater.*, *16*, 1005.

[17] Liu, X., Ly, J., Han, S., Zhang, D., Requicha, A., Thompson, M. E., & Zhou, C. (2005). *Adv. Mater.*, *17*, 2727.

[18] Wu, T. M., & Lin, S. H. (2006). *J. Polym. Sci. Part A: Polym. Phys.*, *44*, 1413.

[19] Wu, T. M., & Lin, S. H. (2006). *J. Polym. Sci. Part A: Polym. Chem.*, *44*, 6449.

[20] Chen, Y. S., Li, Y., Wang, H. C., & Yang, M. J. (2007). *Carbon*, *45*, 357.

[21] Kendall, J. L., Canelas, D. A., Young, J. L., & DeSimone, J. M. (1999). *Chem. Rev.*, *99*, 543.

[22] Watkins, J. J., Blackburn, J. M., & McCarthy, T. (1999). *J. Chem. Mater.*, *11*, 213.

[23] Ye, X. R., Lin, Y., Wang, C. M., & Wai, C. M. (2003). *Adv. Mater.*, *15*, 316.

[24] Dai, X., Liu, Z., Han, B., Sun, Z., Wang, Y., Xu, J., Guo, X., Zhao, N., & Chen, J. (2004). *Chem. Commun.*, *2190*.

[25] Yue, B., Wang, Y., Huang, C. Y., Pfeffer, R., & Iqbal, Z. (2007). *J. Nanosci. Nanotechnol.*, *7*, 1.

[26] Do, K. M., Yuvaraj, H., Woo, M. H., Kim, H. G., Jeong, E. D., Johnston, K. P., & Lim, K. T. (2008). *Colloid Polym. Sci.*, *286*, 1343.

[27] Kim, M., Hong, C. K., Choe, S., & Shim, S. E. (2007). *J. Polym. Sci. Part A: Polym. Chem.*, *45*, 4413.

[28] Ramanathan, T., Fisher, F. T., Ruoff, R. S., & Brinson, L. C. (2005). *Chem. Mater.*, *17*, 1290.

[29] Ma, P. G., Kim, J. K., & Tang, B. Z. (2006). *Carbon*, *44*, 3232.

[30] Tian, B., & Zerbi, G. (1990). *J. Chem. Phys.*, *92*, 3892.

[31] Tan, K. L., Tan, B. T. G., Kang, E. T., & Neoh, K. G. (1992). *J. Mater. Sci.*, *27*, 4056.

[32] Feng, W., Bai, X. D., Lian, Y. Q., Liang, J., Wang, X. G., & Yoshino, K. (2003). *Carbon*, *41*, 1551.